Recent trends and variabilities of convective parameters relevant for hail events in Germany and Europe

S. Mohr *, M. Kunz

Institute for Meteorology and Climate Research (IMK-TRO), Karlsruhe Institute of Technology (KIT), Karlsruhe, Germany
Center for Disaster Management and Risk Reduction Technology (CEDIM), Karlsruhe and Potsdam, Germany

Keywords:
Convective parameters
Trend analysis
Thunderstorms
Hail
Data homogeneity
Climate change

A B S T R A C T

This study investigates whether any evidence can be found to support the occurrence of alterations in the hailstorm frequency in the last few decades (1978 2009) over Germany and Europe. Due to their local scale extent and a lack of appropriate monitoring systems, hailstorms are not captured reliably and comprehensively over long periods by current observation systems. To overcome this constraint, we consider various convective indices and parameters (CPs) derived from soundings at 1200 UTC, and we evaluate which of them are appropriate for predicting hail damage days according to loss data from a building insurance company.

Most of the CPs that rely on moisture at the near surface layers exhibit a significant positive trend towards a higher convective potential. This finding applies to the 90% (10%) percentiles of the annual distribution and to the number of days that exceed (or fall below) a specific threshold, which is suitable for hailstorm prediction. Negative and, at most stations, insignificant trends of CPs that rely on moisture at higher levels or if the initial parameters of the lifting curve were mixed over the lowest layers can be attributed to inconsistency in the time series of the dew point. This in homogeneity is caused by changes in the instrumentation around the year 1990. The investigations show considerable spatial differences in the convective potential both in the mean and the trends, with a distinct north to south gradient and a less marked west to east gradient over Europe and Germany. The spatial distribution of the trends, however, is fairly consistent among the CPs that are based on the same principles.

1. Introduction

Hail is a short lived extreme weather event related to severe thunderstorms. These storms occur frequently in Central Europe in countries such as Germany, Switzerland and France. Hailstorms often cause substantial damage to buildings, crops, automobiles and power lines on the order of several million EUR. In the federal state of Baden Württemberg in southwest Germany, for example, almost 40% of all damage to buildings by natural hazards is currently caused by large hailstones with diameters in excess of 2 cm.

In several regions of Central Europe, damage caused by hail substantially increased during the last two to three decades. Based on loss data of an agricultural insurance company in Switzerland (1920 1999), Schiesser (2003) reported a substantial increase in the number of hail events between 1980 and 1994. Based on insured building damage in southwest Germany, Kunz et al. (2009) detected a significant increase in the number of hail damage days over the last two decades. From hail pad data over France between 1989 and 2009, Berthet et al. (2011) detected an increase in hail intensity by 70%, while the frequency did not change

* Corresponding author at: Institute for Meteorology and Climate Research, Karlsruhe Institute of Technology (KIT), Wolfgang-Gaede-Str. 1, 76131 Karlsruhe, Germany. Tel.: +49 721 608 43565.
E-mail address: mohr@kit.edu (S. Mohr).

significantly during that period. Over Ontario, Canada, Cao (2008) identified a robust ever increasing frequency of severe hail events over the last decades based on damage data. The question arises to what extent this increase in hail damage is driven by changes in exposure or vulnerability or by changes in atmospheric properties, particularly in light of global warming (IPCC, 2007). Alterations in the environmental lapse rate due to differential warming may also modify atmospheric stability. Furthermore, enhanced evaporation in the wake of temperature increases may lead to higher moisture content at low levels and therefore, to an increase in convective energy.

Due to their local scale extent in combination with insuffi cient monitoring systems, hailstorms are not completely and uniformly recorded by meteorological observations, which hampers reliable statistical analysis of the temporal variability and possible long term changes of these storms (Schuster et al., 2005). An alternative approach is to use proxies that are available over a long term period to estimate the occurrence of these events. In effect, the problem is transformed from depending on insufficient observations to establishing a sound relationship between well observed meteorological variables and hailstorm occurrence.

A pre convective environment can be identified and classified, in principle, by convective parameters and indices (hereinafter referred to as CPs) that are assumed to reflect the convective potential of the atmosphere. Various studies have investigated the utility and skill of CPs to predict thunder storms (e.g., Huntrieser et al., 1997; Haklander and van Delden, 2003; Manzato, 2003; Doswell and Schultz, 2006; Sánchez et al., 2008; Kaltenböck et al., 2009). Most of these studies report a relationship between thunderstorm occurrence and appropri ate CPs derived from either radiosonde observations or model simulations. Even if this relation may not be valid for single events, it can be established to quantify the probability of thunderstorm occurrence in the mean.

However, only a few studies have investigated long term variability, including trends in extreme values of CPs that are most appropriate for thunderstorm or hailstorm prediction. DeRubertis (2006), for example, observed significant trends in four common CPs determined from sounding data in the US over a 50 year period. The most consistent spatial patterns with a decrease in atmospheric stability were found over the Great Plains and the southern US states. Cao (2008) related changes in atmospheric convective instability and precipitable water derived from reanalysis data to the observed frequency of severe hail events in Ontario, Canada. He also demonstrated that severe hail events occur more frequently in a warming climate. According to the study of Gensini (2008), based on reanalyses, convective energy increased since the late 1960 over central US, whereas it decreased over other regions, such as South America. Over southwest Germany, Kunz et al. (2009) found that most of the commonly used CPs that depend upon surface temperature and moisture feature positive trends regarding both the annual extremes and the number of days above/below specific thresholds. They concluded that the trend directions of the CPs may be attributable to differential temperature and moisture stratification in the various atmospheric layers.

Our primary goal in this paper is to examine whether any changes in the CPs suggest an increase in the thunderstorm potential in the past 30 to 50 years over Germany and Europe. We focus on the detection of environments associated with the occurrence of severe hail with diameters in excess of 2 cm. Relationships between sounding derived CPs and hail damage days determined from loss data from a building insurance company were evaluated by categorical verification for a mesoscale test region located in southwest Germany. In this process, the CPs that are the most appropriate for predicting damage related hailstorms, including their thresholds, are identified. Because a crucial point in trend analyses is the homogeneity of the samples, we tried to identify possible break points of the time series prior to statistical analyses. Afterwards, various hailstorm related CPs are statistically analysed with respect to linear trends and their statistical significance and stability. The results are discussed with respect to the characteristics of the CPs and the break points identified as the most important in the datasets.

The paper is structured as follows: Section 2 presents the data sets, convective parameters and statistical methods. Section 3 examines the temporal homogeneity of the long term series and uncertainty resulting from gaps in the time series. Section 4 establishes a relation between convective parameters and hail events using categorical verification. The climatology and linear trends of various CPs are discussed in Section 5 for Germany and in Section 6 for Europe. Finally, the last Section 7 highlights the main results and offers some conclusions.

2. Data and methods

The pre convective environment is described by various CPs derived from radiosonde observations at 1200 UTC for the summer half year from April to September, when severe hailstorms occur almost exclusively (Kunz and Puskeiler, 2010). Long term changes are inferred through a linear regression model.

2.1. Sounding data

Radiosonde data available on main pressure levels and significant levels, where one of the variables features a strong gradient, were interpolated into equidistant increments of $\Delta z = 10$ m. Only soundings that reached a minimum pressure level of 200 hPa and a minimum of 15 data points were considered in this study.

Seven sounding stations distributed over Germany and operated by the German Weather Service [Deutscher Wet terdienst (DWD)] were used in the analysis (see Fig. 1, A G, and Table A.4 in the Appendix A). These stations have been continuously in operation at the same location at least between 1978 and 2009. This 32 year period, hereinafter referred to as C20, is considered primarily in the trend analyses. The Schleswig (A) and Stuttgart (F) stations have been in operation the longest (from 1957 onwards) and are thus used for the examination of long term variability. Data from the years 1972 and 1973 are incomplete and available only at levels below 500 hPa. Thus, these two years were discarded in the analysis, and the percentiles considered in the trend analysis were linearly interpolated between the previous and subsequent year. The loss of data, in cluding measurement errors, is between 1.1 and 3.2% for the German soundings, that is, 2 and 6 days per year on average, respectively.

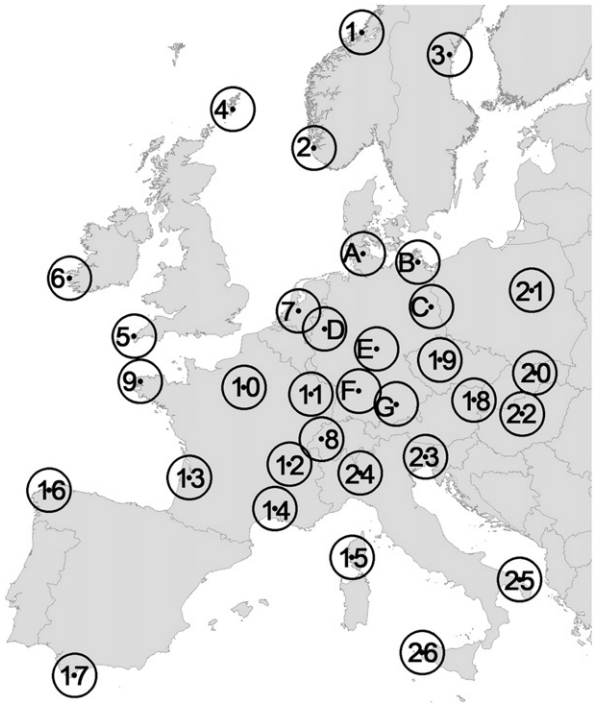

Fig. 1. Sounding stations in Germany (A–G) and Europe (1–26) with an assumed detection radius of 100 km according to Haklander and van Delden (2003).

In addition to the German soundings, 26 stations distributed over Europe from 37.9 to 63.7°N and from −10.3 to 21°E were used for comparison purposes (see Fig. 1, 1 26 and Table A.4). These data were provided by the Integrated Global Radiosonde Archive (IGRA) for quality controlled radiosonde and pilot balloon observations (Durre et al., 2006) at the National Climatic Data Center (NCDC). At most of the stations, reliable moisture data are available only after 1971. Thus, the European analyses are restricted to the period 1971 2009. Unfortunately, several stations exhibit a high percentage of data loss between 5 and 20%. At the De Bilt (7) station, the majority of data in 1999 are not available. As for the German soundings, the CP percentiles are simply interpolated from the previous and following years.

2.2. Insurance loss data

To assess the prediction skill of the various CPs, we used additional hail damage data from a building insurance company recorded between 1986 and 2008. Usually, buildings are damaged by hail with a diameter in excess of 2 cm. It is obvious that these data are restricted to settled regions and influenced by vulnerability. However, these data represent the only available information about severe hailstorm occurrences, and are mostly comprehensive over a longer period. Building insurance against natural hazards was mandatory in Baden Württemberg until 1994 and was offered exclusively by a monopolist. The insurance data of the successor, the "SV SparkassenVersicherung AG" (hereinafter referred to as SV), thus exhibits a high areal coverage and consistency. The SV data comprise for each of the 1236 five digit postal code zones the date, the insured loss and the number of notification of claims. Additional inventory data in terms of number of contracts and insured values allow for a data correction to account for the annual variability of the portfolio, especially for the decrease in the number of contracts after the abolition of the insurance obligation in 1994. In 2008, approximately 70% of all buildings were insured by the SV (in a total of 1,962,385 claims).

In the evaluation of the CP's skill to predict hailstorms, a day was considered a hail day when more than ten claims were settled in a region that is restricted to a 100 km radius from the Stuttgart sounding site (for more details see Kunz, 2007). This definition gives a total of 377 hail damage days within the 23 year period, i.e. 16.4 events on average per year. The time series of hail damage days show a strong increase and a high annual variability between 4 and 31. In the study of Kunz et al. (2009), a relationship was established between those hail days and specific CPs, yielding correlation coefficients between 0.65 and 0.80.

2.3. Convective parameters and indices (CPs)

Various CPs allow for the quantification of atmospheric stability and may be used as predictors for the development of thunderstorms, their probability and intensity (e.g., Galway, 1956; Miller, 1972; Moncrieff and Miller, 1976; Huntrieser et al., 1997). These parameters rely on temperature and dew point at different levels, sometimes complemented by additional kine matic information in terms of vertical shear of horizontal wind. All convective indices and parameters are briefly described in Table A.5 in the Appendix A.

The theoretical concepts underlying these parameters are to represent conditional and/or latent and/or potential instability. A state is referred to as conditional instability when the environmental lapse rate is between the dry and the moist adiabatic lapse rate on a thermodynamic chart (Haurwitz, 1941). This type is represented by the Vertical Totals (VT). When the actual lapse rate above the level of free convection (LFC) is lower than the moist adiabatic lapse rate, it is referred to as latent instability. In this concept, conditional instability in a relatively dry environment can be caused by a moist air parcel rising from below the LFC. Related parameters comprise the Lifted Index (LI), Showalter Index (SHOW), Deep Convective Index (DCI) and Convective Available Potential Energy (CAPE). Finally, potential instability describes an unsaturated column of air, where the equivalent potential temperature θ_e decreases with height (Emanuel, 1994). If such a column is lifted entirely until saturation, it may become unstable. This concept is represented by the KO Index (KO), $\Delta\theta_E$ Index and Potential Instability Index (PII).

Some CPs also combine the three concepts of stability, including the Total Totals (TT) and modified K Index (K_{mod}). Other indices, such as the Severe Weather Threat Index (SWEAT), Swiss Index (SWISS12) and Severe Weather Param eter (SWP), also consider kinematic properties. The latter is defined as the product CAPE × shear, where shear is the magnitude of the difference between the wind vector at the surface and at 6 km height (WSh_{0-6}). The different versions of CAPE, LI, SWP and DCI are calculated either from near surface values of temperature T and dew point temperature Td, denoted by the subscript X_S, or from values mixed over the lowest 100 hPa, denoted by X_{100}.

2.4. Trend analysis

Trends in the time series of the CPs are inferred through a linear regression, which is applied to the 10% percentiles of the annual probability density function (pdf) of LI, KO and SHOW and to the 90% percentiles of all other CPs, such as CAPE, DCI, or $\Delta\theta_E$ (note that the convective potential increases with decreasing values for the former, whereas it is the reverse for the latter). We fitted a pdf to the annual samples of daily CPs (sample size is 183 assuming no data loss) to avoid random scatter of the data at the tail. In the case of CAPE, LI, SHOW, KO and SWP, the best results in terms of the least scatter between data from the sample and inferred from the pdf were obtained with the Gamma distribution

$$y \quad f(x|a,b) \quad \frac{1}{b^k\Gamma(k)}x^{k\ 1}e^{\frac{-x}{b}} \qquad \text{for } x\geq 0, \tag{1}$$

where x is the random variable, $\Gamma(k)$ is the well known Gamma function and k and b are shape and scale parameter, respectively (Wilks, 1995).

All other CPs are described statistically by a Weibull distribution

$$y \quad f(x|a,b) \quad \frac{k}{b}\left(\frac{x}{b}\right)^{k\ 1}e^{\ \left(\frac{x}{b}\right)^k} \qquad \text{for } x\geq 0. \tag{2}$$

To test the statistical significance of the linear trends, the non parametric Mann Kendall (MK) test is applied (Mann, 1945; Kendall and Gibbons, 1955). As shown by von Storch and Narvarra (1995) and Yue et al. (2002), positive serial correlation in the time series increases the variance of the MK statistic, which, in turn, increases the probability for detect ing a significant trend.

A powerful method to account for autocorrelation in the time series is the trend free pre whitening (TFPW) approach, developed by Yue et al. (2002). Four steps are necessary in this process. First, the slope β of a trend inherent in the sample is computed by the non parametric trend slope estimator according to Sen (1968):

$$\beta \quad \text{median}\left(\frac{X_j - X_l}{j-l}\right), \ \forall\ l<j, \tag{3}$$

where X_l and X_j are the lth and jth index values, respectively. This approach is more robust compared with the conven tional linear regression using the least squares method. The trend β, assumed to be linear, is removed from the original time series X_t:

$$X'_t \quad X_t - \beta\cdot t, \tag{4}$$

where t is the time (years). Afterwards, the lag 1 serial correlation coefficient α is calculated from the series X'_t. If no correlation is found, the MK test is directly applied to the original time series. Otherwise, α is removed from the series:

$$Y'_t \quad X'_t - \alpha\cdot X'_{t\ 1}. \tag{5}$$

This step results in a residual series Y'_t without trend and autocorrelation, referred to as the detrended series. In the last step, the trend β according to Eq. (3) is again added:

$$Y''_t \quad Y'_t + \beta\cdot t. \tag{6}$$

The result is a blended series Y''_t, including the original trend, but without any autocorrelation, on which the MK test can be applied. As shown by Bayazit and Onoz (2007), the TFPW method has to be applied when the sample size is small ($n \leq 50$), the trend is low ($\beta \leq 0.01$), and the power of the test is small.

3. Homogeneity of the time series

Temporal homogeneity of the data is a fundamental pre requisite in trend analysis. The potential inhomogeneities examined in this section for the German soundings may result from changes in instrumentation, sounding characteristics (e.g., solar radiation corrections) and gaps in the time series.

3.1. Detection and analysis of change points

Metadata of the soundings are available from both DWD (März, 2010, DWD, personal communication) and IGRA (see metadata by IGRA; Gaffen, 1993). This informa tion, however, is inconsistent and differs regarding the specified year of a change in several cases. Because the temperature measurements can be assumed to be mostly robust, our focus is on changes in the moisture profiles due to different measure ment systems in terms of hygrographs, hygristors or dew point mirrors. Usually, the soundings are initialised by an adjacent ground based station, for example, a synoptic station, where the moisture measurement is much more reliable. Thus, possible inhomogeneities of the sounding data are restricted to higher levels.

The time series of the dew point temperature (1200 UTC, averaged over the summer half year) at five different heights are investigated: 2 m, 950 hPa, 900 hPa, 850 hPa and 700 hPa. In the first step, these series are compared with the metadata with respect to changes in the radiation correction routine and instrumentation as reported by both DWD and IGRA. During most of the period, the time series at the different levels are almost parallel, as observed by the examples of Munich and Schleswig (Fig. 2). However, a few abrupt changes, referred to as change points (ChPos), can be identified. All of the clearly visible ChPos correspond to an instrumentation change. Radiation correction, on the other hand, seems to be of minor importance. At the station of Schleswig, for example, a substantial decrease in *Td* after 1991 is found at all levels, except at 2 m. In particular, the temporally increasing spread between the surface and the 950 hPa level is a strong indication of a break in homogeneity. However, when potential ChPos can be identified at all levels, even in the 2 m data provided by the adjacent synoptic station, they are assumed to be driven by changes in atmospheric conditions and not caused by any artificial change. Such changes are the negative peaks in 1962 at Schleswig or in 1984 at Munich, which occurred at all levels.

To statistically investigate the most important changes listed in the metadata, the nonparametric Wilcoxon signed rank test

(5% level, two sided) was applied to the time series of *Td* from all stations. This test compares mean values obtained from two different time series (Wilks, 1995). Following Gaffen et al. (2000), we split the original time series in the year of a potential ChPo and extracted two 5 year subseries, one before and one after that point. According to the results listed in Table 1, most of the ChPos identified as significant occurred at higher levels. Only a few ChPos can be detected in *Td* at 2 m. The abrupt change in Schleswig in 1991 discussed above is clearly detected by the test. Around this year, similar significant ChPos can be identified at the other stations. These substantial changes coincide with a consistent replacement by the commonly used Väisälä RS80 sonde, which has a faster measuring device and thus gives lower humidity at a certain level (see also Elliott and Gaffen, 1991; Elliott et al., 1994). For example, Miloshevich et al. (2009) detected a dry bias of up to 20% in the middle troposphere (700 hPa) for recent sounding within the three decades. This underestimation, however, affects only CPs that consider moisture at higher levels. CPs that rely on near surface values, such as $CAPE_S$ or $\Delta\theta_E$ are only marginally affected by these changes (see Section 5). The transition from the RS80 to the RS92 sondes at the German stations between 2004 and 2007 according to Steinbrecht et al. (2008) is detected as a ChPo at Schleswig, Meiningen, Stuttgart and Munich. The effect, however, is much less compared with the former replacement.

To further assess the impact of the ChPos on the various CPs, we modified the well known Weisman and Klemp (1982) vertical profile. While the *T* profile was kept constant, the *Td* profile was lowered by the average gradient quantified 5 years before and after the 1991 ChPo at Schleswig. This modification results in a substantial decrease in convective energy; for example, $CAPE_{100}$ decreased from 1042 J kg^{-1} to 610 J kg^{-1}, while LI_{100} increased from −4.4 K to −3.1 K. These changes are greater than the trends discussed in Section 5.2. Even if the 1991 ChPo at Schleswig was that with the highest magnitude and the Weisman and Klemp (1982) profile is far from being a representative of the 90% (10%) percentiles, this assessment shows that CPs including moisture at higher levels are not very reliable. Only CPs that consider dew point or the equivalent potential temperature at the lowest levels are marginally affected by these changes.

3.2. Gaps in the time series

At several stations, in particular those situated outside of Germany, the overall loss of data is considerable (cf. Table A.4), with a relative fraction between 1.1% (Schleswig, Stuttgart and Munich) and 20.2% (Milano). Apart from the observation problems in 1972 and 1973 described in Section 2, the days with data loss or failures are more or less equally distributed over the summer half years.

To estimate the impact of data loss on the percentiles of the annual distribution, we imposed artificial data gaps on the time series of LI_{100} in Schleswig, which is the longest and most complete dataset ($n = 51$ year, without the years 1972/73). An additional data loss of 2, 5, 10 and 20% was accomplished by a Monte Carlo simulation that was repeated $j = 1000$ times. In this process, single data points were excluded from the annual distribution by stochastically generating random numbers according to the selected fraction of losses. This approach yields j different time series, from which $j \times n$ percentile values (10%) of the annual distribution and j linear trends were estimated.

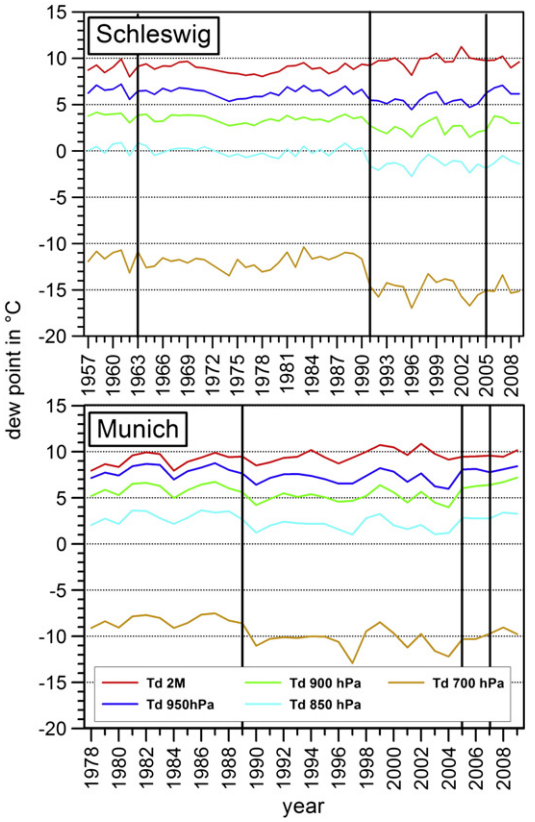

Fig. 2. Time series of mean (summer half-year, 1200 UTC) dew point temperature (Td) at different pressure levels in Schleswig (top) and Munich (bottom); vertical lines indicate changes in the instrumentation.

The distribution of the 10% percentiles, visualised by boxplots in Fig. 3 (top right), appears to be exceptionally robust to data losses. These distributions, however, comprise all $j \times n$ percentiles, thus hiding the spread between the j different time series. In the linear trend estimates, however, the uncertainty due to the simulated data losses is clearly visible by the width of the distributions (Fig. 3). For example, a 2% loss, which is representative for the German soundings, yields a linear trend

Table 1
Change points in the time series of dew point temperature at different levels detected by application of the Wilcoxon signed-rank test for German soundings (1 = ChPo, 0 = no ChPo).

Station	Year	Surface	950 hPa	900 hPa	850 hPa	700 hPa
Schleswig	1991	1	1	1	1	1
	2005	0	1	1	1	0
Greifswald	1993	0	0	1	1	1
Lindenberg	1992	0	0	0	1	1
Essen	1989	0	1	1	1	1
Meiningen	1992	1	1	0	0	1
	2006	0	1	1	1	1
Stuttgart	1990	1	1	1	1	1
	2007	1	1	1	1	1
Munich	1989	0	1	1	1	1
	2005	0	1	1	1	0

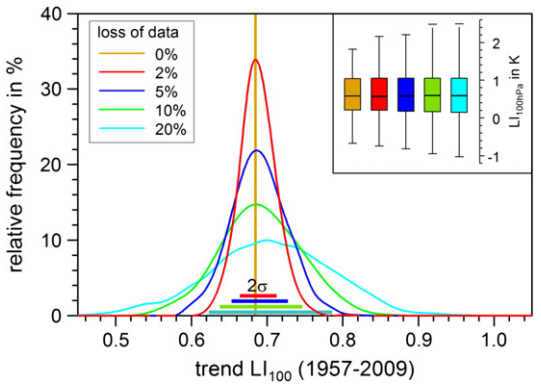

Fig. 3. Histogram of linear trends of LI_{100} in Schleswig due to loss of data imposed by a Monte-Carlo simulation. The small subfigure shows boxplots of the 10% percentiles with interquartile range (box), median and extremes (horizontal lines).

of $\beta = 0.688 \pm 0.024$ K (mean $\pm \sigma$, assuming a normal distribu tion). The uncertainty is substantially lower than the trend value and, thus, can be neglected. For a loss of 20% ($\beta = 0.704 \pm$ 0.081 K), however, the width of the distribution substantially increases, particularly affecting the tails at both sides. Even if the trend in this case is still positive for all j series, its range is extremely large, with values between $\beta = 0.45$ and 0.95. The simulations confirm that it is not possible to draw robust conclusions from series with a high amount of data losses in excess of 5 10%. This fact must be kept in mind when interpreting the estimated trends. The German soundings with a relative loss between 1.1 and 3.2%, however, can be regarded as reliable.

4. Selection of convective parameters

This section identifies convective indices and parameters, including the thresholds (predictors) that are most suitable for predicting hailstorm occurrence (predicant) in the period of 1986 2008. The CPs derived from the Stuttgart soundings are evaluated against hail damage days according to the SV data for a region within a radius of 100 km around the station. This radius was suggested, for example, by Haklander and van Delden (2003) to provide a sound representation of the convective indices. Based on categorical verification using a 2×2 contingency table, various accuracy measures and skill scores, such as the Probability of Detection (POD), False Alarm Rate (FAR), Critical Success Index (CSI), Heidke Skill Score (HSS; Heidke, 1926) and True Skill Statistic (TSS; Hanssen and Kuipers, 1965), were computed. Ideally, the scores for HSS, TSS, POD and CSI should be close to unity, whereas FAR should be reduced to zero. Our ranking of the CPs is based on an optimisation approach using HSS, which is most suitable for events with a low probability (Doswell et al., 1990). Because HSS may reach a kind of plateau within the range of the turning point, where it is less sensitive to small variations of the parameter compared with FAR (Fig. 4), the optimal threshold is determined by

$$\zeta_{thres} \quad \max\{\mathrm{HSS}(\zeta) \pm 0.04\} \cap \min\{\mathrm{FAR}\}, \tag{7}$$

ensuring a low FAR in addition to a high HSS.

The results obtained for all CPs, including their ranking, are listed in Table 2. The highest HSS is obtained for the two versions of LI and for two calculation methods of CAPE. These results agree well with the findings of Manzato (2003) and Kunz (2007) for hailstorms and of Haklander and van Delden (2003) and Pineda and Aran (2011) for thunderstorm prediction.

Even if most of the mixed layer versions of CPs based on a lifted parcel (CAPE, LI, DCI, SWP) perform slightly better compared with the surface based equivalents, a general rule cannot be deduced from this performance. The differences between the two versions of DCI, for example, are only marginal. A robust finding, however, is the significantly lower optimal threshold for the mixed layer CPs simply due to the elimination of a possible superadiabatic stratification at the lowest layers by vertical lifting. Two of the CPs that include additional kinemat ics, SWISS12 and SWEAT, exhibit a very low skill. Only SWP performs better; this parameter, however, is substantially dominated by the CAPE but exhibits a lower HSS compared with the latter. Additionally, convective inhibition (CIN) combined with CAPE does not increase the prediction skill and is therefore not further considered. A modified version of the CAPE according to Manzato (2003), integrated only up to a temperature of -15 of the lifted parcel, also failed to improve the results.

To test the robustness of the findings, the optimisation approach described above was applied additionally to different data sets: (i) shorter time series of the CPs without ChPos to evaluate the effect of inhomogeneities (see Section 3.1), (ii) time series without frontal passages (detected by a decrease in the equivalent potential temperature θ_e of more than 10 K) to exclude changes in ambient conditions not captured by the 1200 UTC soundings, and (iii) damage data from a crop insurance company (Vereinigte Hagelversicherung VVaG) between 2000 and 2009 to account for less severe hail events (most crop damages are caused by small hail). Overall, the results are approximately the same for all different data sets. This finding confirms that the ranking of the CPs, including their optimal thresholds, are relatively robust.

To further minimise the number of CPs that will be considered in the trend analysis and to identify specific characteristics, daily CPs were compared with each other. For this purpose, we used the nonparametric rank correlation coefficient r after Spearman (Wilks, 1995) and applied it to the composite time series, including all soundings between 1957/ 1978 and 2009 (Table 3). The negative values of r indicate that one of the two CPs assumes higher convective potential for decreasing values (LI, SHOW, KO, SWISS12).

Several relationships and redundancies amongst the vari ous CPs can be identified that are mostly independent of the underlying convection concept. As expected, most apparent of these is the high correlation between CAPE and SWP for both versions, with $r = 0.97$ and 0.99, respectively. Furthermore, the mixed versions of CAPE and SWP exhibit correlations that are nearly identical to the other parameters displayed. This relationship is a clear indication that SWP is primarily dominated by the CAPE and only marginally by the shear. Furthermore, a high correlation is also found between LI_{100} and SHOW or KO, respectively. Despite that LI is incorporated into DCI, the two parameters are mostly unrelated ($r = -0.41$ and -0.53), which implies that temperature and moisture at the 850 hPa level are the primary drivers of DCI compared with LI.

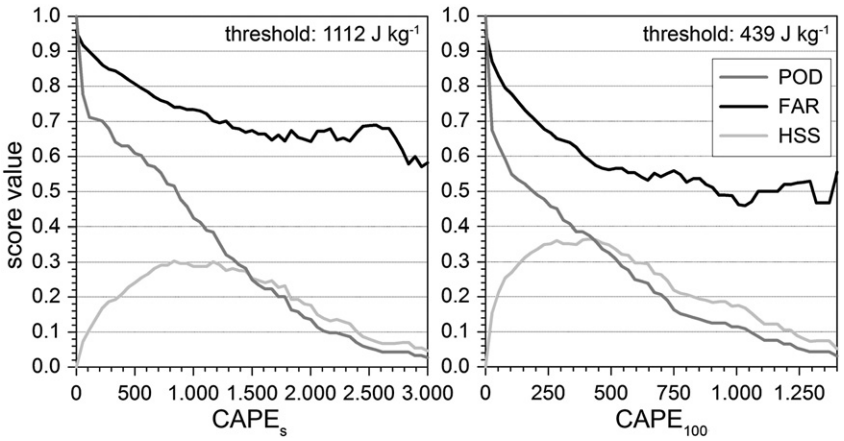

Fig. 4. Skill score values as a function of $CAPE_s$ and $CAPE_{100}$ obtained from the Stuttgart soundings, verified for hail damage days according to SV data within a 100 km radius.

Regarding the origin of the lifted parcels for CPs describing latent instability, it is apparent that the mixed CPs are well related to the surface based equivalents. Most notable are the high correlation coefficients between DCI_S and DCI_{100} ($r = 0.98$) and between LI_S and LI_{100} ($r = 0.90$). This result may suggest that superadiabatic stratification at the lowest layers, often occurring in the summer months, controls the magnitude of the parameters, whereas the overall stability estimate is controlled by the layers aloft. On the other hand, the two versions of CAPE exhibit significantly lower correlation ($r = 0.66$). This result can be explained by the air parcels mixed over the lowest 100 hPa having a temperature/moisture that is too low to overcome the CIN and to reach the LFC, whereas parcels starting from the surface may reach the LFC. For example, 15% of all days at the Stuttgart station have $CAPE_{100} = 0$, while at the same time, $CAPE_S > 0$.

Table 2
CPs with optimal thresholds and different accuracy measures (POD, FAR, CSI) and skill scores (HSS, TSS) for hailstorm prediction verified with SV data and ranked according to HSS.

CP	Threshold	HSS	TSS	POD	CSI	FAR
LI_{100}	≤ 1.6 K	0.39	0.33	0.35	0.27	0.44
$CAPE_{100}$	≥439	0.35	0.26	0.28	0.24	0.41
$CAPE_{10}$	≥721	0.34	0.29	0.32	0.24	0.51
LI_S	≤ 3.6 K	0.34	0.31	0.36	0.24	0.57
PII	≥1.7 K km^{-1}	0.34	0.29	0.32	0.24	0.53
DCI_S	≥26.6 K	0.34	0.29	0.32	0.24	0.54
DCI_{100}	≥24.6 K	0.34	0.29	0.32	0.24	0.53
$\Delta\theta_E$	≥6.2 K	0.33	0.28	0.32	0.23	0.55
SWP_{100}	≥2733 m^3 s^{-3}	0.32	0.25	0.26	0.22	0.45
$CAPE_{CCL}$	≥1978	0.31	0.25	0.27	0.21	0.50
$CAPE_{mul}$	≥1057	0.30	0.29	0.34	0.22	0.62
$CAPE_S$	≥1112	0.30	0.27	0.32	0.21	0.61
KO	≤ 6.3 K	0.29	0.26	0.30	0.20	0.61
SHOW	≤ 0.4 K	0.28	0.22	0.25	0.19	0.54
SWP_S	≥7925 m^3 s^{-3}	0.27	0.23	0.26	0.19	0.59
K_{mod}	≥39.3 K	0.24	0.22	0.26	0.17	0.66
Td_S	≥15.8	0.23	0.22	0.27	0.17	0.69
SWISS12	≤ 1.3	0.18	0.19	0.26	0.14	0.76
VT	≥28.5 K	0.17	0.20	0.30	0.14	0.79
TT	≥50.9 K	0.14	0.16	0.25	0.12	0.81
SWEAT	≥231	0.11	0.09	0.12	0.09	0.77

Based on the relationships found in the analysis, we focused on seven CPs with the highest prediction skill that rely on different stability concepts and constructions of the parcel's lifting curves: $CAPE_S$, $CAPE_{100}$, LI_S, LI_{100}, DCI_S, $\Delta\theta_E$ and PII. However, due to several inhomogeneities identified in the time series, special attention is given to surface based CPs. To further account for possible changes in the kinematics, we additionally consider WSh_{0-6} in the analyses.

5. Temporal variability of CPs in Germany

5.1. Climatology of CPs

To discuss the long term trends in the CPs selected in the previous section, it is useful to understand their climatology with respect to regional differences. The climatological chart (Fig. 5) shows boxplots of LI_{100} during C20: one is obtained from all daily values of the summer half year ($= 183 \times 32 = 5856$ values assuming no data loss), the other from the 10% percentiles of the annual distribution ($= 32$ values). The two boxplots show a distinct north to south gradient and a less marked west to east gradient. Over the most southern stations of Stuttgart and Munich, the atmosphere exhibits the lowest stability, both in the mean and for the extremes. In contrast, the highest stability appears in the northern parts at the stations of Schleswig and Greifswald, reflecting the influence of the Atlantic and the Baltic Sea. At Schleswig, for example, the interquartile range of the 10% percentiles is completely positive, ranging from 0.1 to 1.0 K, with a median of 0.7 K. By contrast, the range at Stuttgart is completely negative (−1.1 to −0.6 K), with a median of −0.8 K, which is approximately 1.5 K lower than Schleswig. The regional differences shown in Fig. 5 for LI_{100} are reflected through almost all CPs considered (see Table A.6 in the Appendix A). The sequence of the mean 90% (10%) percentiles shows a good agreement between the CPs, all reflecting the lowest convection potential for the Schleswig station and the highest for Munich. From the CP climatology, it can be assumed that severe thunderstorms occur most frequently and with the highest intensity over southern Germany.

Table 3
Correlation coefficients between daily CPs from all soundings (Stuttgart and Schleswig: 1957–2009; C20 for all others). Bold numbers indicate $r \geq 0.7$.

	$CAPE_S$	$CAPE_{10}$	$CAPE_{100}$	LI_S	LI_{100}	SHOW	DCI_S	DCI_{100}	K_{mod}	KO	PII	$\Delta\theta_E$	SWISS12	SWEAT	SWP_S
$CAPE_{10}$	**0.86**														
$CAPE_{10}$	0.66	**0.78**													
LI_S	-0.40	-0.32	-0.17												
LI_{100}	-0.49	-0.45	-0.34	**0.90**											
SHOW	-0.41	-0.38	-0.32	**0.71**	**0.87**										
DCI_S	0.39	0.33	0.31	-0.41	-0.54	-0.59									
DCI_{100}	0.34	0.31	0.33	-0.34	-0.53	-0.59	**0.98**								
K_{mod}	0.42	0.46	0.46	-0.49	-0.66	**-0.72**	0.48	0.49							
KO	-0.36	-0.32	-0.19	**0.75**	**0.83**	**0.74**	-0.28	-0.24	-0.45						
PII	0.38	0.37	0.43	-0.06	-0.25	-0.28	0.66	0.68	0.29	0.10					
$\Delta\theta_E$	**0.73**	0.52	0.39	-0.18	-0.21	-0.18	0.61	0.51	0.20	-0.08	0.45				
SWISS12	-0.43	-0.44	-0.34	0.45	0.55	0.56	-0.22	-0.21	-0.66	0.42	-0.09	-0.11			
SWEAT	0.31	0.35	0.39	-0.28	-0.43	-0.55	0.41	0.42	0.53	-0.30	0.22	0.14	-0.47		
SWP_S	**0.97**	**0.83**	0.65	-0.35	-0.44	-0.37	0.37	0.32	0.41	-0.31	0.33	0.51	-0.44	0.36	
SWP_{100}	0.65	**0.77**	**0.99**	-0.16	-0.33	-0.30	0.31	0.33	0.45	-0.18	0.41	0.36	-0.35	0.41	0.66

5.2. Long term changes in CPs

Long term changes in the pre convective environment are investigated using the 90% (10%) percentiles of the annual distribution of all CPs considered. These percentiles are assumed to better reflect the thunderstorm potential of the atmosphere than the median or annual mean.

An example is shown in Fig. 6 with a time series (1957 2009) including linear trends of the two versions of CAPE at the Schleswig station. Despite the high annual variability, exhibits a significant positive trend of $335 \pm 116\ J\ kg^{-1}$. This trend is primarily caused by the strong increase over the last 15 years. Prior to that increase, a kind of plateau can be observed with fluctuations of approximately $300\ J\ kg^{-1}$. By contrast, the overall trend of $CAPE_{100}$ is negative, with $-57 \pm 40\ J\ kg^{-1}$. As discussed in Section 3.1, a significant break in the time series due to instrumentation change was identified in 1991 at Schleswig, leading to a higher gradient in *Td* of approximately 1.9 K between the surface and 950 hPa. This change coincides with a substantial decrease of $60\ J\ kg^{-1}$ in the time series of $CAPE_{100}$, which partly explains the overall negative trend. However, no jump can be identified for. Furthermore, this figure illustrates the difficulty of interpreting the trends in the CPs. Both convective energy measures, $CAPE_S$ and $CAPE_{100}$, exhibit a comparatively high prediction skill for hail damage days, as confirmed by HSS = 0.30 and 0.35, respectively (see Section 4). Their trends, however, are opposite, at least when considering the whole time period of 53 years.

For LI and CAPE during C20, the situation is approximately similar in Germany in terms of trend directions (Fig. 7). The surface based parameters, and, show a trend towards higher convective potential. At five of the seven stations, this trend is statistically significant (>90% according to MK statistics); only at the two stations in the northeast the significance is below 90%. Regarding the magnitudes of the trends, a north to south gradient can be detected, as was already found in the climatological means and extremes (cf. Fig. 5). The Stuttgart station features the highest trend of $\Delta LI_S = -2 \pm 1.2$ K and $\Delta = -671 \pm 361$ (see Table A.6 for more details). In contrast, the trends of the mixed layer CPs, $CAPE_{100}$ and LI_{100}, are negative at most of the stations.

Trends comparable to those analysed for CAPE and LI are also found for the other CPs (Fig. 8, left). Most of the CPs with a significant trend show an increase towards higher convective potential. This increase is obvious particularly for the stations in the southern parts of Germany (Essen, Meiningen, Stuttgart and Munich) for the CPs of and already discussed, and for DCI_S and $\Delta\theta_E$. The results for Lindenberg are similar, but significant positive trends are also detected for DCI_S, PII and $\Delta\theta_E$ (but not for $CAPE_S$ and LI_S). Only a few CPs at the stations in the north show significant reverse trends. The most conspicuous is the

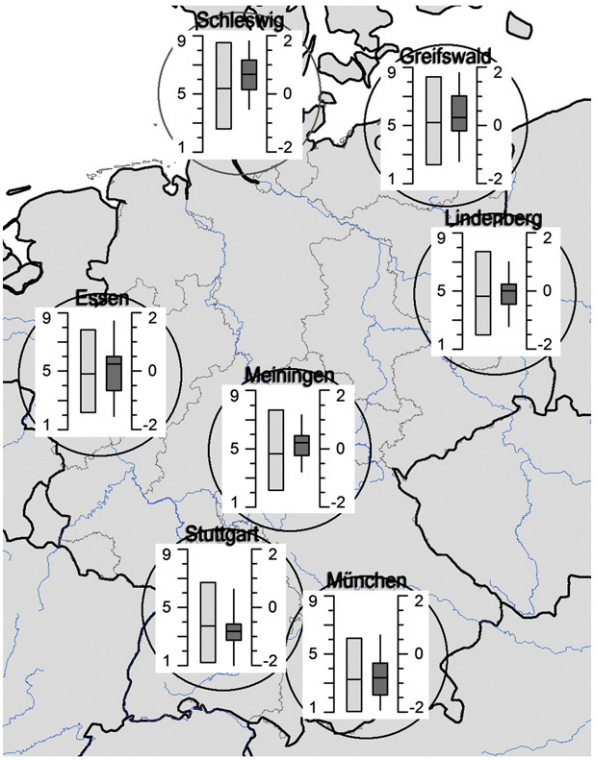

Fig. 5. Boxplots of LI_{100} (in K) showing the interquartile range and median at the sounding stations of Germany from daily values (light grey) and 10% percentiles (dark grey; with min/max values) in C20. The launching position is located in the middle of the circles that indicate a detection radius of 100 km.

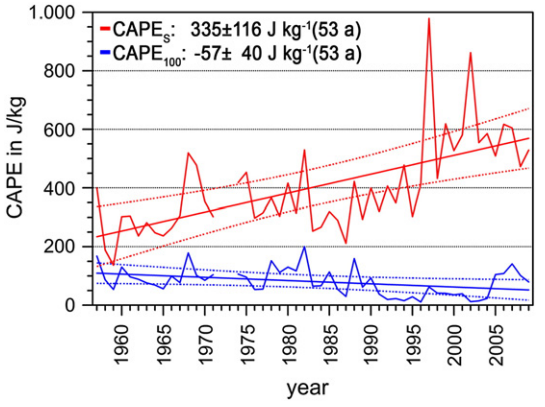

Fig. 6. Time series (1957 to 2009) of the 90% percentile of two CPs ($CAPE_S$ and $CAPE_{100}$) at the Schleswig station; indicated are linear trends (solid) with 95% confidence intervals (dashed).

Greifswald sounding, where $CAPE_{100}$ and LI_{100} feature signif icant trends towards higher stability.

In summary, whereas the trends over northern Germany are ambiguous, the different CPs over the central and southern parts suggest an increase in the convective potential during C20. All CPs considering near surface temperature and moisture indicate an increase in the convective potential. Most of the CPs that are computed from temperature and dew point at higher levels or mixed over the lowest 100 hPa in the boundary layer feature a decrease. Regarding the concept of static stability in terms of latent, conditional, or potential instability, no systematics are found. The same is true for the parameters considering kinetic properties, WSh_{0-6}, SWISS12 and SWEAT (the latter two are not shown).

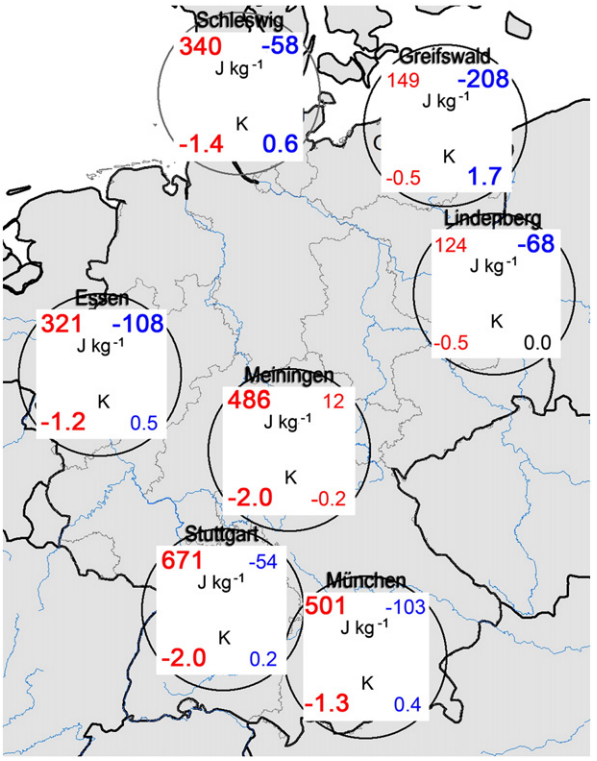

Fig. 7. Linear trends during C20 for the 90% percentiles of $CAPE_S$ (subfigure top left), $CAPE_{100}$ (top right), LIS (bottom left) and LI_{100} (bottom right). Large bolt numbers indicate significant trends (>90%), smaller numbers insignificant trends.

The different trend directions can be explained physically by different trends in temperature and moisture at the various layers (Fig. 8, right). While the temperatures at all levels show positive trends, which are statistically significant at various low levels in the south, the increase in the mixing ratio (or dew point temperature) is restricted to the surface, with values between 0.5 and 1.5 g kg^{-1}. At higher levels, however, slight decreases can be detected at most of the stations. At 500 hPa, the overall trend is negative, particularly due to the ChPos in the time series approximately 1990 (see Section 3.1).

To focus not only on the trends in the various CPs but also to consider possible changes in the number of potential hail days, we determined all days within a year that exceed (or fall below) a certain threshold (see Table 2). Note that the thresholds were determined for the Stuttgart sounding and SV data, which explains the decreasing magnitude of the trends in the south to north direction. In general, the results shown in Fig. 9 are similar to the trends of the 90% (10%) percentiles of the CPs (Fig. 7). At most of the stations, the number of days that exceed the threshold for $CAPE_S$ exhibit a significant increase (insignificant at Greifswald and Lindenberg) between 4.9 (Schleswig) and 16.7 days (Stuttgart). A similar result is apparent for LI_S. In contrast but in accordance with the percentiles the number of days above/below the thresholds of the two mixed parameters, $CAPE_{100}$ and LI_{100}, show an insignificant decrease for most of the stations.

5.3. Trends in variable time series

The high temporal variability of the CP time series (see Fig. 6) may give completely different trends when consider ing other time periods. Therefore, we evaluate in this section the robustness of the trends to shifts in the time series computed from the 90% (10%) percentiles of CAPE, LI (both surface based and mixed), $\Delta\theta_E$, PII, and WSh_{0-6}. In our analyses, we considered the two stations of Stuttgart and Schleswig, where data are available over $n = 53$ years. As shown in the previous section, these two stations represent the more continental climate in the south and the more maritime climate in the north of Germany. By incrementally truncating the original time series up to a minimum length of 11 years and shifting these both forward and backward in time, we extracted $j = 1 + 2 + \ldots + (n - 10) = 946$ subseries. The results in terms of linear trends and statistical significance (level $\geq$90%) computed for each subseries are displayed by means of trend matrices. Each point in the trend matrix (Fig. 10) indicates the trend per year computed from the sample that begins in the year shown on the x axis and ends in the year on the y axis. For example, the points marked in the matrices are the trends for the C20 time series discussed in the previous section.

Regarding the directions and significance of the trends, it is obvious that the matrices reflect the high temporal variability of the time series discussed in the previous sections. The majority of the trends estimated from all 946 time series displayed in each matrix are insignificant, particularly for and PII, but also for WSh_{0-6}. Most of the subseries representing mixed CP versions, $CAPE_{100}$, LI_{100} and PII, show a trend towards a lower convective

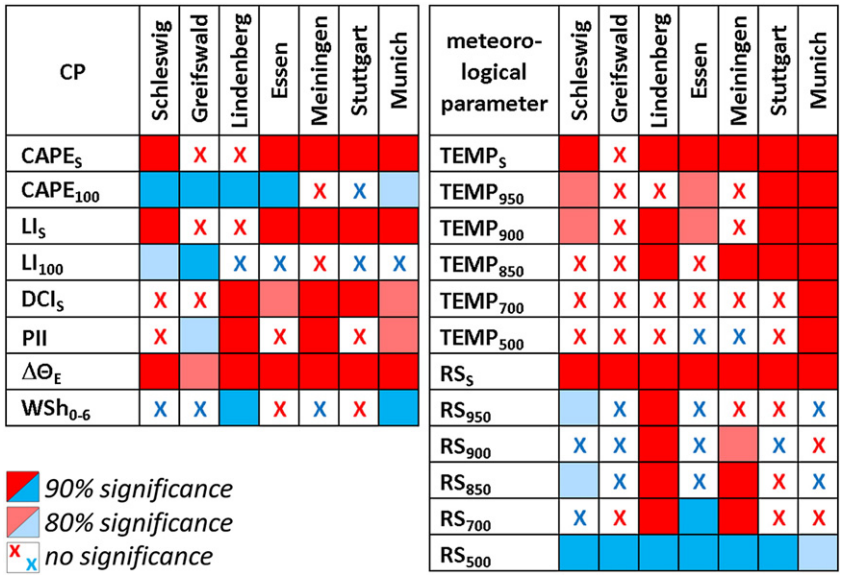

Fig. 8. Linear trends during C20 including significance estimates for various CPs (left) and meteorological parameters (TEMP = temperature, RS = mixing ratio) at several pressure levels (right). Red colours indicate a decrease in stability (increase in TEMP/RS), blue colours an increase in stability (decrease in TEMP/RS). Trend values are also listed in Table A.6 in the Appendix A.

potential. Positive trends can be detected particularly in the time series after the identified ChPo in 1991 (cf. Section 3.1). In the period before that ChPo, the mixed CPs are nearly identical to the surface based versions with deceases and increases, depending on which station is considered. According to the surface based CPs, $CAPE_S$, LI_S and $\Delta\theta_E$ the convective potential at both stations significantly increased during most of the time series that end after 2000. The same is found for the series of the last two decades. This time period, however, is too short to draw any conclusions from; rather, it can be interpreted as an indication that the convective potential has changed in recent years.

The highest values of the trends are found for the period after 1990 at both observation sites. Between 1990 and 2000 at Stuttgart, for example, exhibits a trend of approximately 60 per year, leading to an overall increase of $+600\ J\ kg^{-1}$. This substantial enhancement over a short period also illustrates the potential lack in robustness of trends derived from highly variable time series. Depending on whether such a strong increase (or decrease) is included in a longer time series or not, the overall trend may change its direction or, at least, its statistical significance. This is the reason why the trend directions for all CPs change several times during the whole period. However, the quantified trends are found to be robust against small shifts in the time periods. This result holds true particularly for the C20 series discussed in the previous section. Large gradients in the trend values occur only infrequently. In these cases, they are usually restricted to short record lengths of approximately 10 years and are statistically insignificant.

At the Stuttgart station, the magnitudes of the trends are substantially higher than those at Schleswig. The highest value at Schleswig is $40\ J\ kg^{-1}$, whereas it is approximately three times greater in Stuttgart, at $141\ J\ kg^{-1}$. The same applies to the other CPs, regardless of whether mixing is considered or not. These differences are consistent with the climatology (cf. Fig. 5), and they confirm a relationship between the trend magnitudes and the mean (extreme) values. While Schleswig indicates an increase in the convective potential according to CAPE and LI for most of the time series of the first three decades, it is the reverse for Stuttgart (except for the small peak from 1963 to 1975). This result may also explain the higher trends at Stuttgart at the end of the investigation period. Furthermore, most of the negative

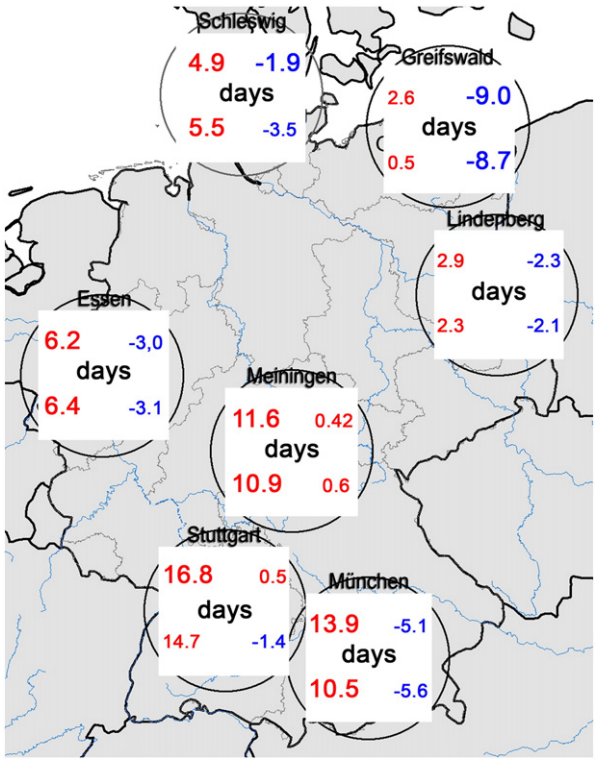

Fig. 9. Same as Fig. 7, but for the number of days per year that exceed thresholds of $CAPE_s \geq 1112\ J\ kg^{-1}$, $CAPE_{100} \geq 439\ J\ kg^{-1}$, $LI_s \leq -3.6\ K$ and $LI_{100} \leq -1.6\ K$.

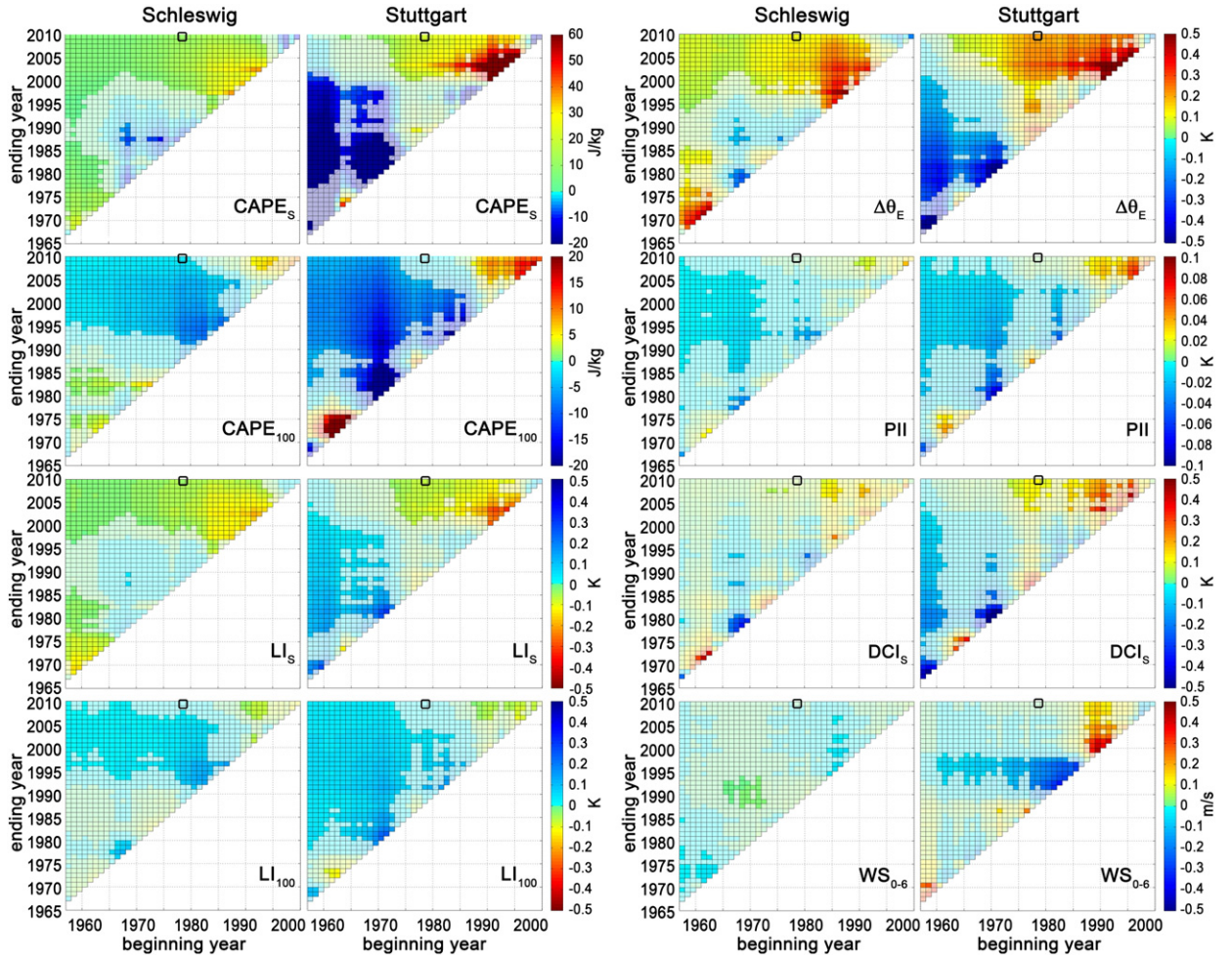

Fig. 10. Trend matrices showing linear trends per year (90/10%-percentile) for different CPs derived from the Schleswig and Stuttgart soundings. The x-coordinate represents the beginning year, the y-coordinate the ending year. Trends with a significance below 90% are brightened. Green to red colours indicate an increase in the convective potential, while blue colours indicate a decrease (note that the colour bars are inverted for the CPs, where the convective potential increases with decreasing values). The small boxes indicate the trends for C20.

trends at Schleswig are statistically insignificant, such as the series beginning between 1965 and 1982 and ending between 1975 and 1995. This relationship between trend direction and significance, however, does not hold true at Stuttgart.

6. Temporal variability of CPs over Europe

6.1. Climatology of CPs

As for the German soundings, we begin our investigation of the CPs over Europe with a discussion of the climatology of convective instability during C20. The boxplots of LI_{100} showing the mean values and 10% percentiles of the annual distribution reveal considerable spatial differences, with a pronounced north to south gradient and a weakly pro nounced west to east gradient (Fig. 11). These gradients were already identified in the climatological chart for Germany (Fig. 5). Stable conditions in the 10% percentiles are represented by the stations in the north, for example, Orland (1) and Lerwick (4), with medians of 100 = 2.4 K and 3.6 K, respectively. By contrast, the highest convective instability is found over northern Italy [Udine (23) and Milano (24)], with negative medians of the 10% percentiles of 100 = −2.3 K and −2.0 K, respectively. Soundings with a completely negative interquartile range of the extremes are restricted to an area that is located south of a line extending approximately from La Coruña in Spain (16) to Legionowo in Poland (21). The high correlation between the medians of both distributions ($r = 0.98$) is an indication that the statistical distributions of LI_{100} from all stations are qualita tively similar regardless of the location.

6.2. Long term changes in CPs

From all European soundings, where data are available over at least 30 years in C20, linear trends, including their statistical significance, were computed from the 90% (10%) percentiles of the annual distribution of various CPs. Recall that data loss is high at several stations; thus, the results should be interpreted carefully. As examples, Fig. 12 depicts the trends of $CAPE_S$ and $CAPE_{100}$. In general, the results are similar to those of Germany. Most of the stations reveal a significant increase in between 145

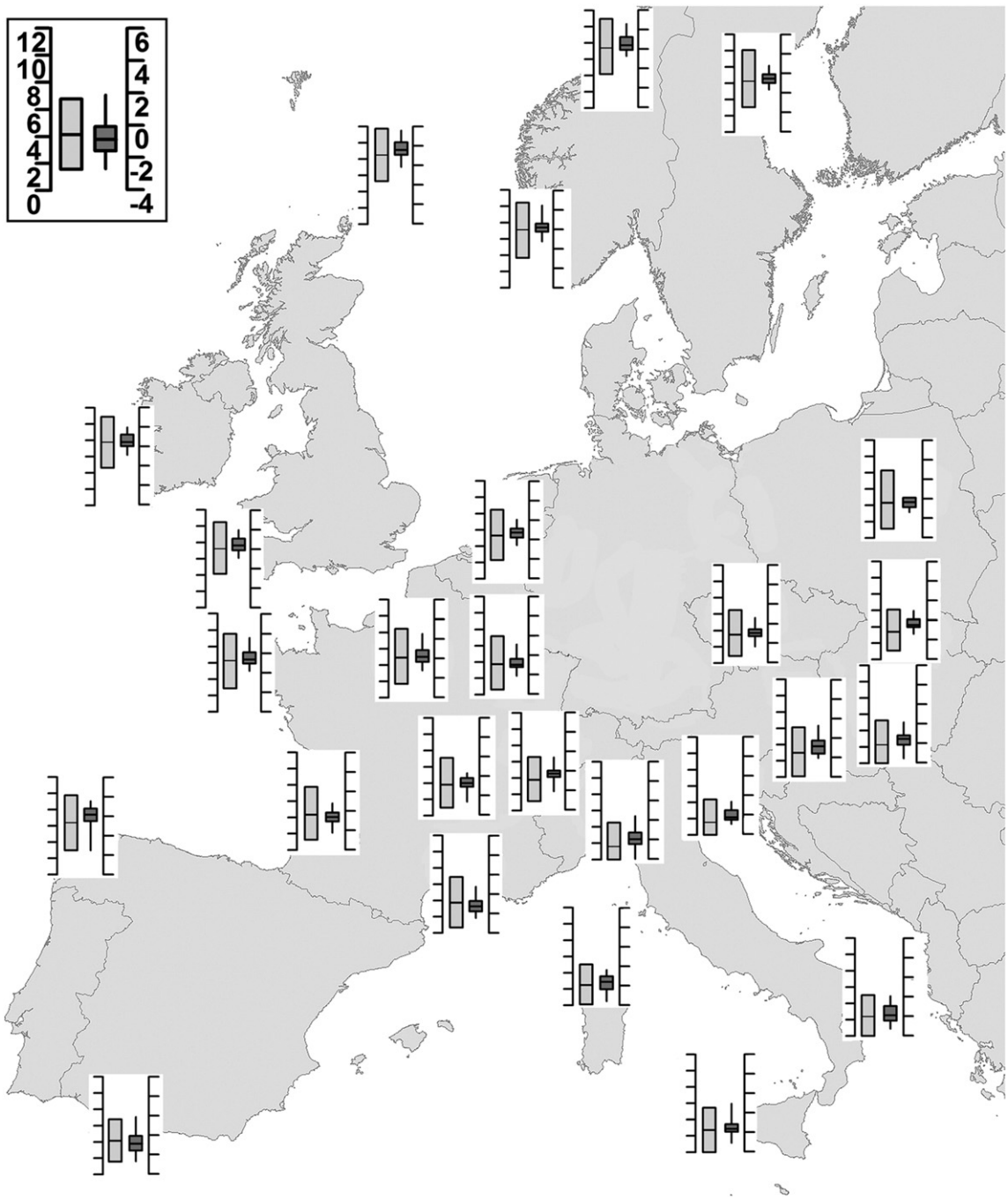

Fig. 11. Same as Fig. 5, but for European soundings outside of Germany for C20 (except for the stations 2 and 11, where data are available only from 1978 to 2008, see Table A.4). The scale on the top left refers to all boxplots in the Figure.

and 1354 J kg^{-1}. Significant positive trends on the order of 500 J kg^{-1} are found among several stations in Europe, with only a few exceptions. Given the dependence of high values on temperature and moisture near the surface, these changes are not unexpected, particularly at stations with a more continental climate. Although an increase in the convective energy can be observed at most of the Central European stations, a distinctive regional pattern is not found. The highest significant trends of more than 1000 J kg^{-1} appear in Vienna [Austria (18)] and at two stations in Italy [Milano (24) and Trapani (26)].

The trends in $CAPE_{100}$, however, are negative at most of the stations, but statistically insignificant. Only four stations situated in north Germany and Gibraltar (19) feature negative significant trends. By contrast, three stations in the central and eastern parts of Europe (20, 21, 24) reveal a significant increase in $CAPE_{100}$. However, for $CAPE_S$, no clear regional pattern related to the

climatology or to specific features of the surrounding terrain can be established.

Considering all CPs over Europe, several similarities can be detected, as well as distinctions, with regard to the spatial patterns of the trends and their significance. Overall, the CPs that rely on near surface temperature and moisture, $CAPE_S$, LI_S, $\Delta\theta_E$ and show significant positive trends toward enhanced instability at most of the locations (upper row in Fig. 13). Only a few stations feature slightly negative trends, but these are statistically insignificant (<80%). One exception, for example, is Udine (23) in northern Italy, which was already identified as having the highest convective potential of all European soundings (see Section 6.1). Due to the high percentage data loss of 19.4% at this station, the computed trend is not very reliable.

For comparison, the CPs that rely on mixed lowest layers (CAPE100 and LI_{100}), show unevenly distributed trend directions, which are insignificant at most locations (Fig. 13, bottom). In particular, CAPE100 features significant trends only at one third of all 33 stations. As discussed for Germany, the European sondes were replaced by the Väisälä RS80 sonde around the year 1990 (Gaffen et al., 2000). Therefore, it can be assumed that the ChPos related to this instrumentation change are responsible for the insignificant trends in the cases of mixed CPs (cf. Section 3.1).

Considering the physical concept underlying the formulation of the different CPs, some relations can be detected. For example, a relation exists between $\Delta\theta_E$ and $CAPE_S$, which are based on latent instability without vertical mixing. The agreement of the trends between CAPE and LI indicates that atmospheric stability beyond the 500 hPa level is of minor importance for estimating convective energy. This conclusion was already drawn from the high correlation of the parameters derived for German sites and confirmed by the trend matrices in Section 5.3. Here, it is verified by a high number of soundings.

It should be noted that the trend matrices determined from the subseries of the European soundings (not shown)

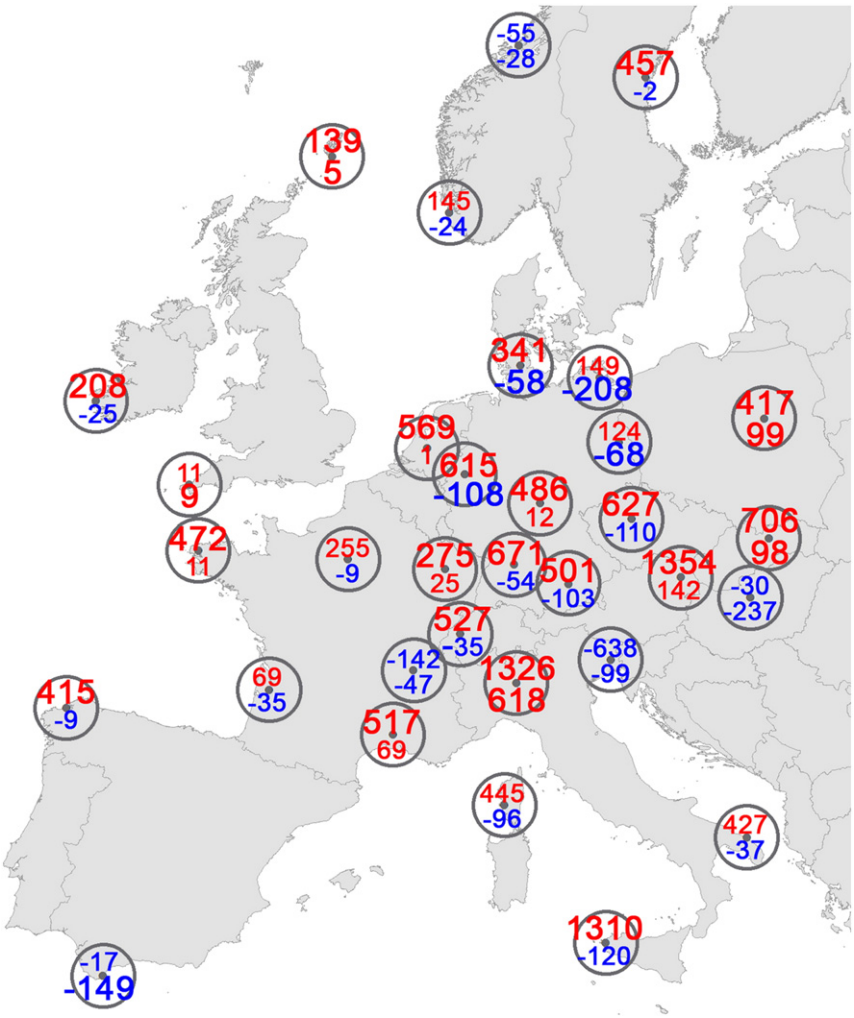

Fig. 12. Linear trends during C20 for the 90% percentiles of $CAPE_s$ (top within the circle) and $CAPE_{100}$ (bottom). Large bolt numbers indicate significant trends (>90%), smaller numbers insignificant trends.

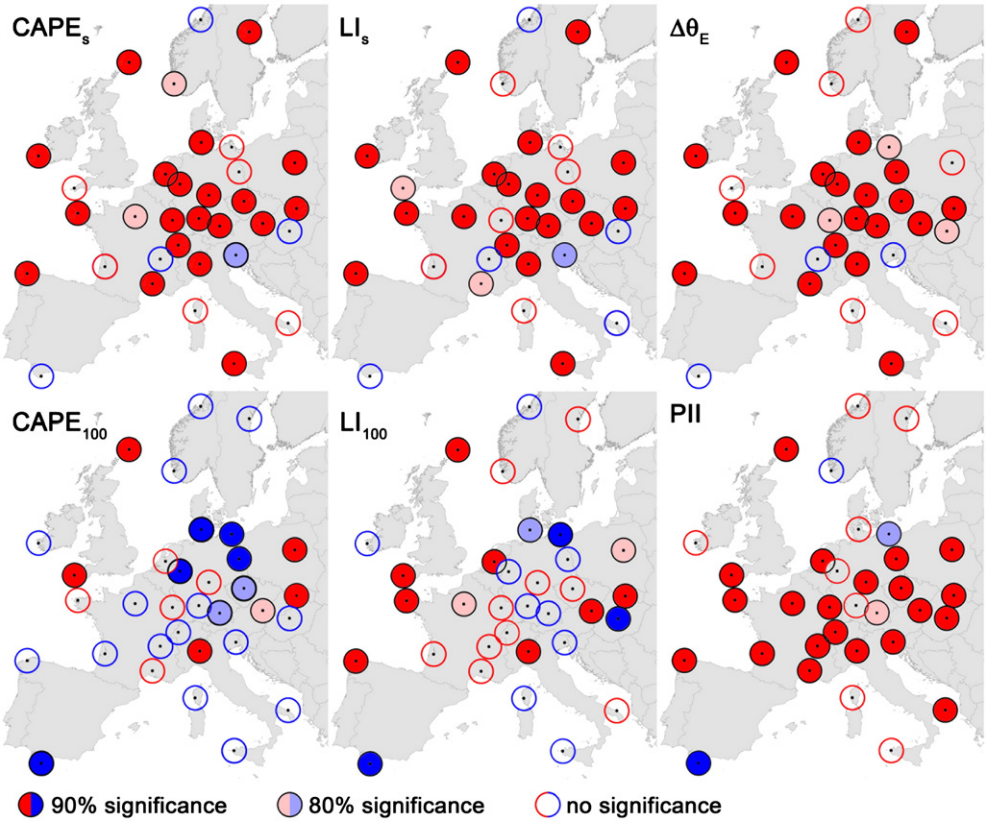

Fig. 13. Linear trends during C20 for the 90% (10%) percentiles of the CPs indicated in the subfigures. The colour definition is the same as in Fig. 8.

approximately reflect the results of the German soundings (cf. Fig. 10). The period for which the data are analysed statistically is the most decisive for the magnitude and the significance of the trends. For example, the station of Gibraltar (17) in Spain and the stations of Bordeaux and Nîmes (13 and 14) in France exhibit high positive trends for the periods from 1977/1983 to 1994, whereas in the last three decades, a negative trend is analysed. However, the trend matrices of neighbouring stations are often similar in magnitude, which provides some confidence that the results of the trend analysis are reliable at most of the stations.

In summary, the spatial distribution of positive or negative trends is fairly consistent among the CPs that are based on the same principles. When considering only significant trends, an increase towards higher convective potential predominates for most CPs calculated from near surface values. In contrast, CPs that rely on the mixed lowest layers seem to be severely affected by inhomogeneities of the time series, which mostly affects moisture at higher levels.

7. Discussion and conclusions

This study examines whether there is evidence suggesting changes in the convective potential related to hailstorms during the last few decades (1978 2009) over Germany and Europe. Because hail is not captured accurately by current observation systems over a long period, the investigations are based on various convective parameters derived from radiosonde obser vations. In the first step, we identified possible breaks in the time series of dew point caused by instrumentation changes and the impacts on the CPs. The effect of data loss on the linear trend is estimated using a Monte Carlo simulation. For a mesoscale test region, where additional insurance data are available, we investigated which of the various CPs predict hail damage days best by using categorical verification. Based on the CPs with the highest prediction skill, the climatological means and trends in the convective potential over the last three (to five) decades were examined. To consider extreme events that are most decisive for hailstorms, the analyses in terms of linear trends and statistical significance are based on the 90% (10%) percentiles of the annual distribution of the various CPs. Additionally, different time periods are considered to evaluate the stability of the trends.

From the results obtained in this study, the following major issues and conclusions are inferred:

1. The atmosphere has become more unstable over the last two to three decades over both Germany and Central Europe. Most of the CPs determined from temperature and moisture at the lowest layers exhibit a positive trend that is significant at the 90% level. This result applies to the 90% (10%) percentiles of the annual distribution and the number of days that exceed (or fall) below a specific threshold that is appropriate for the prediction of hailstorms. The spatial distribution of the trends is fairly

consistent among the CPs that are based on the same principles. Negative, but in most cases insignificant, trends of CPs that consider moisture at higher levels or mixed over the lowest levels can be assigned to change points in the observed time series of the dew point caused by instrumentation changes. These breaks also explain the discrepancies between the trends derived from soundings and those obtained from reanalysis data (ERA 40, dynam ically downscaled by the climate version of COSMO, Mohr and Kunz, 2011). In these simulations, mixed parameters such as $CAPE_{100}$ also show considerable trends towards a higher convective potential.

2. Due to the high annual variability of the CPs, it is necessary to focus not only on a fixed period but also to examine the stability of the trends for variable lengths of the time series. In particular, the trends during 1978 2009 mainly inves tigated in this study are mostly robust against small shifts in time.
3. The convective potential shows considerable spatial dif ferences over Europe, but also over Germany, with a distinct north to south gradient and a less marked west to east gradient. The climatology of convective instability can be understood as a result of the different climates in combination with large scale atmospheric charac teristics. This result agrees well with thunderstorm observations, for example, from cloud overshooting top detections (Bedka, 2011) or lightning detection data (Damian, 2011).
4. A relation can be established between days with damaging hail and appropriate CPs, which means that even if hail is a local scale phenomenon, specific large scale atmospheric conditions are necessary for thunderstorm or hailstorm development. The highest prediction skill is found for the two versions of LI and CAPE. The mixed layer versions of the CPs do not necessarily perform better compared with the surface based equivalents. Thus, no conclusion can be drawn about the layers most decisive for deep convection to develop. Parameters that also include dynamic properties perform worse, except for the product of CAPE and shear, which, however, is dominated by CAPE. This finding is contrary to several studies of severe hailstorms in the US (e.g., Weisman and Klemp, 1982; Brooks et al., 2003). A plausible explanation may be a pre existing flow deviation in the boundary layer caused by the complex orography, which is characteristic for Europe.
5. The vertical profiles of the soundings are significantly affected by instrumentation changes. A major change point in the time series of dew point was identified around the year 1990, where the sondes were replaced at all European stations by the same type, the Väisälä RS80. In the aftermath, humidity substantially decreased at higher levels, whereas it remained mostly constant at low levels (note that the sondes are usually initialised by observa tions at a ground based station). This decrease affects all CPs that rely on higher levels or are mixed over a certain layer, but not the surface based equivalents. However, a data loss in excess of 5 10% may substantially modify the results in terms of trends and significance. Thus, it does not make sense to interpret single sites; rather, the overall picture obtained from the multiplicity of soundings is most decisive in the assessment of the convective potential. This conclusion, however, does not apply to Germany, where the loss of data is small.

Convective parameters derived from soundings have some restrictions. They reflect atmospheric conditions only for a certain location and at a specific time (1200 UTC), which is a few hours before the peak in thunderstorm occurrence. Kunz and Puskeiler (2010), for example, detected the majority of hailstorms over southwest Germany between 1300 and 1600 UTC. When air masses with different properties are advected, for example, in conjunction with a frontal passage, the sounding cannot be representative of the whole area and the whole period. Another limitation of the CPs is that they do not account for forced ascent by large scale lifting or local scale convergence zones, which often trigger deep convection (e.g., Barthlott et al., 2011).

Apart from alterations in the environmental lapse rate due to differential warming, the main driver for the increase in the convective potential is the positive trend in moisture at low levels, which is a prerequisite for convective initiation. Following the Clausius Clapeyron argument, enhanced evap oration in the wake of temperature rise caused by climate change may lead to higher moisture content at low levels and, thus, to a growth in convective energy. This hypothesis is supported by the fact that the surface based relative humidity exhibits no trend at all (not shown). An increase in the lower tropospheric water vapour and the nearly fixed relative humidity are also projected by atmospheric and oceanic general circulation models (Held and Soden, 2006). However, this connection does not explain the high annual to decadal variability found in the CPs. Rather, these fluctua tions may be related to the natural variability caused by the arrangement of the prevailing synoptic systems. As shown in the studies of Kunz et al. (2009) and Kapsch et al. (Submitted for publication), hail related large scale weather patterns exhibit very high temporal variability over Germany. Accord ingly, the rising frequency of specific weather patterns associated with an advection of warm and moist air masses from the southwest might also increase the potential for thunderstorm development.

In the next step, we will consider further parameters, such as moisture fluxes and their horizontal convergence, com bined with synoptic scale lifting (ω fields) from reanalysis data. By applying empirical orthogonal functions (EOF) and logistic regression, we intend to establish a more reliable and robust relationship between hail occurrence of variable intensity and various atmospheric properties. This approach will be transferred and applied to an ensemble of regional climate models (RCMs) to quantify possible changes, includ ing uncertainty assessment of hailstorm potential in the future.

Acknowledgements

The authors thank the SV SparkassenVersicherung for providing the insurance data for Baden Württemberg and the German Weather Service (DWD) and the Integrated Global Radiosonde Archive (IGRA) for providing the sounding data. This work was funded by the “Stiftung Umwelt und Schaden vorsorge”, which we also want to thank.

Appendix A

Table A.4
The sounding stations in Germany (A–G) and Europe (1–26) considered in this study (bold numbers: difference to the standard C20 period (1978–2009)).

	Country	Name	Location	Latitude	Longitude	Altitude [m]	Time period	Outage [%]
1	NO	01241	Orland	63.70	9.60	10	1971–2009	18.4
2	NO	01415	Stavanger/Sola	58.87	5.67	37	1971–**2008**	11.4
3	SW	02365	Timra/Midlanda	62.53	17.45	6	1971–2009	10.0
4	UK	03005	Lerwick	60.13	1.18	84	1971–2009	9.9
5	UK	03808	Camborne	50.22	5.32	88	1971–2009	13.1
6	EI	03953	Valentia	51.93	10.25	30	1971–2009	11.4
7	NL	06260	De Bilt	52.10	5.18	4	1971–2009	11.6
8	SZ	06610	Payerne	46.82	6.95	501	1971–2009	11.4
9	FR	07110	Brest	48.45	4.42	103	1971–2009	14.8
10	FR	07145	Trappes	48.77	2.00	168	1971–2009	14.2
11	FR	07180	Nancy	48.68	6.22	212	1971–**2008**	13.5
12	FR	07481	Lyon	45.73	5.08	240	1971–2009	17.4
13	FR	07510	Bordeaux	44.83	0.68	61	1971–2009	11.2
14	FR	07645	Nimes	43.87	4.40	62	1971–2009	12.6
15	FR	07761	Ajaccio	41.92	8.80	9	1971–2009	11.2
16	SP	08001	La Coruna	43.37	8.42	67	1971–2009	18.8
17	GI	08495	Gibraltar	36.15	5.35	4	1971–2009	9.3
A	GM	10035	Schleswig	54.53	9.55	48	1957–2009	1.1
B	GM	10184	Greifswald	54.10	13.40	6	1978–2009	3.2
C	GM	10393	Lindenberg	52.22	14.12	110	1978–2009	2.6
D	GM	10410	Essen	51.40	6.97	153	1978–2009	2.3
E	GM	10548	Meiningen	50.57	10.38	453	1978–2009	3.0
F	GM	10739	Stuttgart	48.83	9.20	315	1957–2009	1.1
G	GM	10868	Munich	48.25	11.55	489	1978–2009	1.1
18	AU	11035	Wien/Hohe Warte	48.23	16.37	200	1971–2009	14.3
19	EZ	11520	Praha/Libus	50.00	14.45	305	1971–2009	11.7
20	LO	11952	Poprad/Ganovce	49.03	20.32	706	1971–2009	14.8
21	PL	12374	Legionowo	52.40	20.97	96	1971–2009	16.8
22	HU	12843	Budapest/Lorinc	47.43	19.18	140	1971–2009	15.7
23	IT	16044	Udine	46.03	13.18	92	1971–2009	19.4
24	IT	16080	Milano	45.43	9.28	103	1971–2009	20.2
25	IT	16320	Brindisi	40.65	17.95	10	1971–2009	14.9
26	IT	16429	Trapani	37.92	12.50	14	**1976**–2009	19.6

Table A.5
Summary of CPs: T and Td are temperature and dew point temperature, θ_e and θ_w are equivalent potential and wetbulb potential temperature, Z is the geopotential height (gpm) and R_d is the gas constant for dry air ($J(kg\ K)^{-1}$). The subscript indicates a certain constant pressure level; an arrow indicates lifting of an air parcel (e.g., $T'_{x\rightarrow y}$ is the temperature T of a parcel at the y-level, which was initially lifted dry adiabatically from the x-level to its condensation level and moist adiabatically thereafter).

CP	Equation	Reference/comment
A: Indices describing conditional instability		
Vertical Totals	$VT = T_{850} - T_{500}$	Miller (1972)
B: Indices describing latent instability		
Lifted Index	$LI_X = T_{500} - T'_{X\rightarrow 500}$	Galway (1956); starting level for creating the lifting curve from the surface ($X \equiv S$) or mixed over the lowest 100 hPa ($X \equiv 100$)
Deep Convective Index	$DCI_X = (T + Td)_{850} - LI_X$	Barlow (1993)
Showalter Index	$SHOW = T_{500} - T'_{850\rightarrow 500}$	Showalter (1953)
Convective available potential energy	$CAPE_X = R_d \int_{LFC}^{EL} (T'_v - T_v)\ d\ln p$	Moncrieff and Miller (1976); T'_v is the virtual temperature of an air parcel (Doswell and Rasmussen, 1994) lifted from the surface ($X \equiv S$) or mixed over the lowest X hPa to the level of free convection (LFC) up to the equilibrium level (EL). T_v is the virtual temperature of the environment.
	$CAPE_{CCL} = R_d \int_{CCL}^{EL} (T'_v - T_v)\ d\ln p$ $CAPE_{mul} = R_d \int_{i;LFC}^{EL} (T'^{*}_v - T_v)\ d\ln p$	same as above, but the air parcel is lifted moist adiabatically from the convective condensation level (CCL) defined for a parcel with T, Td and p at a level where θ_e reaches its highest value in the lowest 250 hPa

Table A.5 (*continued*)

CP	Equation	Reference/comment
C: Indices describing potential instability		
KO Index	$KO = 0.5(\theta_{e500} + \theta_{e700}) \quad 0.5(\theta_{e850} + \theta_{e1000})$	Andersson et al. (1989); because the local pressure is often below 1000 hPa, we used 950 hPa instead;
Delta-θ_e	$\Delta\theta_e = \theta_{eS} \quad \theta_{e300}$	Atkins and Wakimoto (1991); designed to assess the potential for wet microbursts
Potential Instability Index	$PII = (\theta_{e925} \quad \theta_{e500})/(Z_{500} \quad Z_{925})$	van Delden (2001)
D: Combination of A–C		
Total Totals	$TT = (T + Td)_{850} \quad 2T_{500}$	Miller (1972)
K-Index	$K = (T_{850} \quad T_{500}) + Td_{850} \quad (T \quad Td)_{700}$	George (1960); developed for forecasting air mass thunderstorms
modified K-Index	$K_{mod} = (T^* \quad T_{500}) + Td^* \quad (T \quad Td)_{700}$	Charba (1977); T^* and Td^* calculated by averaging between the surface and the 850 hPa level
E: Indices considering kinematic properties		
SWISS Index	$SWISS12 = LI_s \quad 0.3\ WSh_{0\ 3} + 0.3(T \quad Td)_{650}$	Huntrieser et al. (1997); $WSh_{0\ 3}$ is the wind shear between the surface and 3 km above ground level; the index was designed for the 1200 UTC sounding in Switzerland
Severe Weather Threat Index	$SWEAT = 12Td_{850} + 20(TT \quad 49) + 2f_{850} + f_{500} + 125[\sin(d_{500} \quad d_{850})] + 0.2$	Miller (1972); f and d are wind speed in knots and direction in (0–360°) on the indicated levels; the first two terms must be greater than or equal to zero; the last term is set to zero if any of the conditions are not met: $130° \le d_{850} \le 250°$, $210° \le d_{500} \le 310°$, $d_{500} > d_{850}$ and both f_{850} and $f_{5000} \ge 15$ knots. SWEAT was designed for the prediction of severe thunderstorms
Severe Weather Parameter	$SWP_X = CAPE_X \cdot Wsh_{0\ 6}$	Craven and Brooks (2004); $WSh_{0\ 6}$ is the wind shear between the surface and 6 km above ground level

Table A.6
Trends and statistical significance related to Fig. 8. In each cell, the first row shows the mean of the 90% percentiles during C20, the second row the linear trend and the third row the significance and the upper/lower confidence interval (±). Bold numbers indicate statistical significance >80%.

CP	Schleswig	Greifswald	Lindenberg	Essen	Meiningen	Stuttgart	Munich
$CAPE_s$[J kg ^{1}]	454	575	679	615	556	606	1032
	341	149	124	**321**	**486**	**671**	**t 501**
	(**99.9**%) ± **167**	(64.5%) ± 207	(72.3%) ± 214	(**99.2**%) ± **189**	(**99.9**%) ± **172**	(**99.9**%) ± **361**	(**99.9**%) ± **280**
$CAPE_{100}$[J kg ^{1}]	72	115	128	109	92	171	172
	58	**208**	**68**	**108**	12	54	**103**
	(**96.4**%) ± **58**	(**99.9**%) ± **74**	(**95.4**%) ± **76**	(**96.1**%) ± **73**	(21.7%) ± 61	(62.8%) ± 98	(**82.2**%) ± **110**
LI_s [K]	1.7	2.2	2.7	2.4	2.2	2.6	3.8
	1.4	0.5	0.5	**1.2**	**2.0**	**2.0**	**1.3**
	(**99.9**%) ± **0.8**	(39.6%) ± 0.9	(66.1%) ± 0.8	(**98.0**%) ± **0.8**	(**99.9**%) ± **0.8**	(**99.6**%) ± **1.2**	(**99.8**%) ± **0.8**
LI_{100} [K]	0.7	0.3	0.1	0.1	0.2	0.8	0.8
	0.6	**1.7**	0.0	0.5	0.2	0.2	0.4
	(**86.0**%) ± **0.7**	(**99.9**%) ± **0.8**	(1.3%) ± 0.7	(66.9%) ± 0.9	(46.2%) ± 0.7	(27.9%) ± 0.7	(77.0%) ± 0.8
DCI_S [K]	16.7	18.4	20.7	19.7	21.3	23.1	25.6
	1.5	0.6	**2.3**	**1.5**	**3.2**	**3.4**	**1.7**
	(72.3%) ± 2.2	(21.7%) ± 2.3	(**89.9**%) ± **2.1**	(**84.2**%) ± **2.4**	(**99.1**%) ± **2.3**	(**97.4**%) ± **2.8**	(**85.1**%) ± **2.6**
PII [K km ^{1}]	0.2	0.4	0.6	0.6	0.8	1.2	1.4
	0.0	**0.2**	**0.5**	0.11	**0.5**	0.2	**0.4**
	(6.5%) ± 0.2	(**82.7**%) ± **0.3**	(**99.9**%) ± **0.3**	(21.7%) ± 0.3	(**99.6**%) ± **0.3**	(57.3%) ± 0.3	(**87.3**%) ± **0.4**
$\Delta\theta_E$ [K]	1.0	0.6	2.0	1.4	1.6	2.6	6.1
	3.4	**2.0**	**2.1**	**3.3**	**5.4**	**6.5**	**3.5**
	(**99.8**%) ± **2.1**	(**86.0**%) ± **2.2**	(**93.3**%) ± **2.1**	(**99.1**%) ± **2.1**	(**99.9**%) ± **2.1**	(**99.9**%) ± **2.8**	(**99.8**%) ± **2.2**
$WSh_{0\ 6}$ [m s ^{1}]	13.5	13.4	13.28	14.4	14.4	14.3	14.1
	0.2	0.2	**1.2**	0.1	0.7	0.4	**1.4**
	(38.5%) ± 1.21	(26.7%) ± 1.3	(**94.6**%) ± **1.2**	(49.4%) ± 1.2	(67.7%) ± 1.3	(43.0%) ± 1.1	(**99.7**%) ± **0.9**

References

Andersson, T., Andersson, M., Jacobsson, C., Nilsson, S., 1989. Thermodynamic indices for forecasting thunderstorms in southern Sweden. Meteorol. Mag. 116, 141–146.

Atkins, N., Wakimoto, R., 1991. Wet microburst activity over the southeastern United States: implications for forecasting. Weather Forecast. 6 (4), 470–482.

Barlow, W., 1993. A new index for the prediction of deep convection. Preprints 17th Conf. on Severe Local Storms, St. Louis, MO. Amer. Meteor. Soc, pp. 129–132.

Barthlott, C., Burton, R., Kirshbaum, D., Hanley, K., Richard, E., Chaboureau, J.P., Trentmann, J., Kern, B., Bauer, H.S., Schwitalla, T., et al., 2011. Initiation of deep convection at marginal instability in an ensemble of mesoscale models: a case-study from COPS. Q. J. R. Meteorol. Soc. 137, 118–136.

Bayazit, M., Onoz, B., 2007. To prewhiten or not to prewhiten in trend analysis? Hydrol. Sci. J. 52 (4), 611.

Bedka, K.M., 2011. Overshooting cloud top detections using MSG SEVIRI Infrared brightness temperatures and their relationship to severe weather over Europe. Atmos. Res. 99, 175–189.

Berthet, C., Dessens, J., Sanchez, J.L., 2011. Regional and yearly variations of hail frequency and intensity in France. Atmos. Res. 100 (4), 391–400.

Brooks, H.E., Lee, J.W., Craven, J.P., 2003. The spatial distribution of severe thunderstorm and tornado environments from global reanalysis data. Atmos. Res. 67, 73–94.

Cao, Z., 2008. Severe hail frequency over Ontario, Canada: recent trend and variability. Geophys. Res. Lett. 35 (14), L14803.

Charba, J.P., 1977. Operational system for predicting thunderstorms two to six hours in advance. NOAA. NWS TDL-64. Techniques Development Laboratory, National Weather Service, Silver Spring, MD.

Craven, J.P., Brooks, H.E., 2004. Baseline climatology of sounding derived parameters associated with deep, moist convection. Natl. Weather Dig. 28, 13–24.

Damian, T., 2011. Blitzdichte im Zusammenhang mit Hagelereignissen in Deutschland und Baden-Württemberg. Seminar thesis at the Institute for Meteorology and Climate Research (IMK), Karlsruhe Institute of Technology (KIT), Germany.

DeRubertis, D., 2006. Recent trends in four common stability indices derived from US radiosonde observations. J. Climate 19, 309.

Doswell III, C.A., Rasmussen, E.N., 1994. The effect of neglecting the virtual temperature correction on CAPE calculations. Weather Forecast. 9, 619–623.

Doswell III, C.A., Schultz, D.M., 2006. On the use of indices and parameters in forecasting severe storms. Electron. J. Severe Storms Meteor. 1 (3).

Doswell III, C.A., Davies-Jones, R., Keller, D.L., 1990. On summary measures of skill in rare event forecasting based on contingency tables. Weather Forecast. 5 (4), 576–585.

Durre, I., Vose, R.S., Wuertz, D.B., 2006. Overview of the integrated global radiosonde archive. J. Climate 1151 (19), 53–68.

Elliott, W.P., Gaffen, D.J., 1991. On the utility of radiosonde humidity archives for climate studies. Bull. Am. Meteor. Soc. 72, 1507–1520.

Elliott, W., Gaffen, D., Kahl, J., Angell, J., 1994. The effect of moisture on layer thicknesses used to monitor global temperatures. J. Climate 7 (2), 304–308.

Emanuel, K., 1994. Atmospheric Convection. Oxford University Press, USA.

Gaffen, D.J., 1993. Historical changes in radiosonde instruments and practices: final report. WMO Instruments and Observing Methods Report No. 50, WMO/TD No. 541. World Meteorological Organization, Geneva, Italy.

Gaffen, D.J., Sargent, M.A., Habermann, R.E., Lanzante, J.R., 2000. Sensitivity of tropospheric and stratospheric temperature trends to radiosonde data quality. J. Climate 13 (10), 1776–1796.

Galway, J.G., 1956. The lifted index as a predictor of latent instability. Bull. Am. Meteor. Soc. 37, 528–529.

Gensini, V., 2008. Regional variablity of CAPE and deep shear from reanalysis. 24th Conference on Severe Local Storms, 27–31 October 2008, Savannah, United States.

George, J.J., 1960. Weather Forecasting for Aeronautics. Academic Press, New York, USA.

Haklander, A.J., van Delden, A., 2003. Thunderstorm predictors and their forecast skill for the Netherlands. Atmos. Res. 67–68, 273–299.

Hanssen, A.W., Kuipers, W.J.A., 1965. On the relationship between the frequency of rain and various meteorological parameters. Meded. Verhand. 81, 2–15.

Haurwitz, B., 1941. Dynamic Meteorology. McGraw-Hill Book Company, Ney York, USA.

Heidke, P., 1926. Berechnung des Erfolges und der Güte der Windstärkenvorhersage im Sturmwarnungsdienst. Geogr. Ann. 8, 310–349.

Held, I.M., Soden, B.J., 2006. Robust responses of the hydrological cycle to global warming. J. Climate 19, 5686–5699.

Huntrieser, H., Schiesser, H.H., Schmid, W., Waldvogl, A., 1997. Comparison of traditional and newly developed thunderstorm indices for Switzerland. Weather Forecast. 12, 108–125.

IPCC, 2007. Climate Change 2007: the physical science basis, contribution of working group I to the fourth assessment. In: Solomon, S., Qin, D., Manning, M., Chen, Z., Marquis, M., Averyt, K.B., Tignor, M., Miller, H.L. (Eds.), Report of the Intergovernmental Panel on Climate Change. Cambridge University Press, Cambridge, United Kingdom and New York, NY, USA.

Kaltenböck, R., Diendorfer, G., Dotzek, N., 2009. Evaluation of thunderstorm indices from ECMWF analyses, lightning data and severe storm reports. Atmos. Res. 93 (1–3), 381–396.

Kapsch, M. L., Kunz, M., Vitolo, R., Economou, T., Submitted for publication. Long-term variability of hail-related weather types in an ensemble of regional climate models. Submitted for publication to J. Geophys. Res.

Kendall, M.G., Gibbons, J.D., 1955. Rank correlation methods. Charles Griffin, London, United Kingdom.

Kunz, M., 2007. The skill of convective parameters and indices to predict isolated and severe thunderstorms. Nat. Hazards Earth Syst. Sci. 7, 327–342.

Kunz, M., Puskeiler, M., 2010. High-resolution assessment of the hail hazard over complex terrain from radar and insurance data. Meteor. Z. 19 (5), 427–439.

Kunz, M., Sander, J., Kottmeier, C., 2009. Recent trends of thunderstorm and hailstorm frequency and their relation to atmospheric characteristics in southwest Germany. Int. J. Climatol. 29 (15), 2283–2297.

Mann, H.B., 1945. Nonparametric tests against trend. Econometrica 13 (3), 245–259.

Manzato, A., 2003. A climatology of instability indices derived from Friuli Venezia Giulia soundings, using three different methods. Atmos. Res. 67, 417–454.

März, R., Apr. 2010. personal communication. DWD

Miller, R.C., 1972. Notes on analysis and severe storm forecasting procedures of the air force global weather central. Air Weather Service Tech. Rept 200 (Rev.): Air Weather Service, AWS/XTX, Scott Air Force Base, IL 62225-5438.

Miloshevich, L.M., Vömel, H., Whiteman, D.N., Leblanc, T., 2009. Accuracy assessment and correction of Vaisala RS92 radiosonde water vapor measurements. J. Geophys. Res. , p. 114.

Mohr, S., Kunz, M., 2011. Trend analysis of meteorological parameter relevant to hail from soundings and reanalysis data. 6th European Conference on Severe Storms (ECSS 2011), 3–7 October 2011, Palma de Mallorca, Balearic Islands, Spain.

Moncrieff, M.W., Miller, M.J., 1976. The dynamics and simulation of tropical cumulonimbus and squall lines. Q. J. R. Meteorol. Soc. 102, 373–394.

Pineda, N., Aran, M., 2011. Convective instability indices as thunderstorm predictors for catalonia. 6th European Conference on Severe Storms (ECSS 2011), 3–7 October 2011, Palma de Mallorca, Balearic Islands, Spain.

Sánchez, J.L., López, L., Bustos, C., Marcos, J.L., García-Ortega, E., 2008. Short-term forecast of thunderstorms in Argentina. Atmos. Res. 88 (1), 36–45.

Schiesser, H.H., 2003. Hagel. Extremereignisse und Klimaänderung. Organe consultatif sur les changements climatiques (OcCC), Bern, Swiss, pp. 65–68.

Schuster, S.S., Blong, R.J., Speer, M.S., 2005. A hail climatology of the greater Sydney area and New South Wales, Australia. Int. J. Climatol. 25 (12).

Sen, P.K., 1968. Estimates of the regression coefficient based on Kendall's tau. J. Am. Stat. Assoc. 63 (324), 1379–1389.

Showalter, A.K., 1953. A stability index for thunderstorm forecasting. Bull. Am. Meteor. Soc. 34, 250–252.

Steinbrecht, W., Claude, H., Schönenborn, F., Leiterer, U., Dier, H., Lanzinger, E., 2008. Pressure and temperature differences between Vaisala RS80 and RS92 radiosonde systems. J. Atmos. Oceanic Technol. 25 (6), 909–927.

van Delden, A., 2001. The synoptic setting of thunderstorms in Western Europe. Atmos. Res. 56 (1–4), 89–110.

von Storch, H., Narvarra, A., 1995. Analysis of Climate Variability: Applications and Statistical Techniques, Vol. 334. Springer-Verlag, New York, USA.

Weisman, M.L., Klemp, J.B., 1982. The Dependence of Numerically Simulated Convective Storms on Vertical Wind Shear and Buoyancy. Mon. Weather Rev. 110, 504–520.

Wilks, D.S., 1995. Statistical Methods in the Atmospheric Sciences: An Introduction. Academie Press, San Diego, California, USA.

Yue, S., Pilon, P., Phinney, B., Cavadias, G., 2002. The influence of autocorrelation on the ability to detect trend in hydrological series. Hydrol. Process. 16 (9), 1807–1829.